Runaway dilaton models: Improved constraints from the full cosmological evolution

Léo Vacher[1,2,*] Nils Schöneberg,[3,†] J. D. F. Dias,[4,5,6] C. J. A. P. Martins[4,5,‡] and Francisco Pimenta[4,6]

[1]*Institut de Recherche en Astrophysique et Planétologie, CNRS, CNES, 31028 Toulouse, France*
[2]*Université de Toulouse UPS, 31028 Toulouse, France*
[3]*Department de Física Quàntica i Astrofísica, Institut de Ciències del Cosmos (ICCUB),*
Facultat de Física, Universitat de Barcelona (IEEC-UB), Martí i Franqués, 1, E08028 Barcelona, Spain
[4]*Centro de Astrofísica da Universidade do Porto, Rua das Estrelas, 4150-762 Porto, Portugal*
[5]*Instituto de Astrofísica e Ciências do Espaço, CAUP, Universidade do Porto,*
Rua das Estrelas, 4150-762, Porto, Portugal
[6]*Faculdade de Ciências, Universidade do Porto, Rua Campo Alegre, 4169-007, Porto, Portugal*

One of the few firm predictions of string theory is the existence of a massless scalar field coupled to gravity, the dilaton. In its presence, the value of the fundamental constants of the universe, such as the fine-structure constant, will vary with the time-dependent vacuum expectation value of this field, in direct violation of the Einstein equivalence principle. The *runaway dilaton* proposed by Damour, Piazza, and Veneziano provides a physically motivated cosmological scenario which reconciles the existence of a massless dilaton with observations, while still providing nonstandard and testable predictions. Furthermore, the field can provide a natural candidate for dynamical dark energy. While this model has been previously constrained from local laboratory experiments and low-redshift observations, we provide here the first full self-consistent constraints, also including high redshift data, in particular from the cosmic microwave background. We consider various possible scenarios in which the field could act as quintessence. Despite the wider parameter space, we make use of recent observational progress to significantly improve constraints on the model, showing that order unity couplings (which would be natural in string theory) are ruled out.

I. INTRODUCTION

The discovery of the Higgs boson at the LHC [1,2], confirmed that spin-0 scalar fields are part of the building blocks of nature. As they are easy to couple to gravity without breaking covariance, they are now commonly invoked as a powerful tool to model cosmological paradigms, including quintessence, early dark energy, inflation, symmetry breaking phase transitions (with their associated topological defects), and—last but not least—dynamical varying couplings [3].

Moreover, they appear as a theoretical necessity in most of grand unification scenarios and attempts of building a quantum theory of gravity. This is the case of string theory, one of the most promising paths connecting quantum field theories and gravity (for a review see, e.g., [4]). Indeed, many bridges have already been built between gravity and quantum fields thanks to quantum strings, such as the recent AdS–CFT correspondence and similar applications

of the holographic principle (see, e.g., [5]). Even though it is still impossible to tell what the final form of the theory should be, one of its uncircumventable predictions seems to be the existence of a scalar partner to the graviton field, called the *dilaton*. Its dynamics sets the intensity of the various interactions between strings through the *string coupling*, and therefore that of the fundamental forces of the standard model. Among other things, the evolution of the dilaton field implies a variation of all the fundamental dimensionless couplings, such as the fine-structure constant. In turn, this implies a violation of the Einstein equivalence principle [6,7]).

Theory suggests that the dilaton should be massless, which would be in violent contradiction with observations. To overcome such an issue in a physically motivated manner, it has been proposed that the dilaton coupling to other matter fields is attracted toward finite smooth limits [8–10]. This model is called the *runaway dilaton* and has the advantage of providing clear predictions, that can be confronted with observations. As such, it can be used as a very compelling testbed model to implement and study variations of fundamental constants on cosmological scales. Moreover, with a suitable choice of potential

$V(\phi)$ or extra couplings, the dilaton field can provide a physically motivated source of dynamical dark energy [11].

The present work builds upon several previous phenomenological studies [11–14] while aiming to be more accurate and more general. This is achieved by confronting the full cosmological field evolution with the latest datasets, as done in [15] for Bekenstein models, while freeing ourselves from assumptions made in previous studies. In Sec. II we introduce the evolution equations of the coupled dilaton field, as well as their impact on various observables. In Sec. III we present the datasets we use in order to obtain the constraints discussed in Sec. IV. Finally, we present our conclusions in Sec. V.

II. PHENOMENOLOGY OF THE COUPLED RUNAWAY DILATON

The dilaton field Φ appears in every string and superstring theory as a massless scalar excitation of the bosonic string. It comes as a massless scalar mode on the first exited state of the closed string along with two rank-2 tensor fields: the symmetric metric tensor $\tilde{g}_{\mu\nu}$ and the antisymmetric Neveu-Schwarz B-field $B_{\mu\nu}$, which plays a role comparable to an electromagnetic gauge field for extended objects. As such, Φ is a partner of the graviton and contributes to the behavior of gravity itself (for an elementary introduction see, e.g., [16]). At tree level, it is expected to be coupled to the various sectors in the string-frame Lagrangian through coupling functions $B_i(\Phi)$ with $i = \tilde{g}, F, \psi, \Phi \ldots$. While string theory cannot predict the exact form of these coupling functions, the assumption underlying the *runaway dilaton* model is that they can naturally be attracted toward a finite smooth limit [9] as

$$B_i(\Phi) = C_i + \mathcal{O}(e^{-\Phi}), \qquad (1)$$

this can reconcile a massless dilaton with experimental observations while still providing many nonstandard but observable predictions.

The direct coupling of Φ to gravity is reabsorbed in a conformal transformation of the metric $\tilde{g} \to g$ and a redefinition of the field $\Phi \to \phi$ [8], leading to an effective low energy Lagrangian density in the Einstein frame

$$\mathcal{L} = \frac{R}{16\pi G} + \frac{1}{8\pi G}(g^{\mu\nu}\partial_\mu\phi\partial_\nu\phi - V(\phi))$$
$$- \frac{1}{4}B_{\hat{F}}(\phi)\hat{F}^a_{\mu\nu}\hat{F}^{a\mu\nu} - B_\psi(\phi)\bar{\psi}\not{D}\psi + \ldots, \qquad (2)$$

where R is the Ricci scalar and $\hat{F}$ and ψ are respectively the various gauge field strengths and fermion fields. D are the covariant derivatives including the coupling between fermions and gauge fields. In principle the sum extends infinitely over all the massive modes of the string, and they can potentially be coupled. Note that we adopt the notation of previous literature, in which ϕ is measured in

units of $\sqrt{\hbar \cdot c/(4\pi G)} = m_{\rm pl}/\sqrt{4\pi}$ with the Planck mass $m_{\rm pl} \approx 2.176 \times 10^{-8}$ kg. In particular, the normalization is not the usual $m_{\rm pl}/\sqrt{8\pi}$ used in many other contexts in cosmology, leading to slightly unconventional kinetic energy terms in the Lagrangian of Eq. (2) as well as in Eqs. (3) and (4) below. We set $\hbar = c = 1$.

The field's density and pressure are

$$\rho_\phi = \rho_T + \rho_V = \frac{1}{8\pi G}[\dot{\phi}^2 + V(\phi)], \qquad (3)$$

$$P_\phi = P_T + P_V = \frac{1}{8\pi G}[\dot{\phi}^2 - V(\phi)], \qquad (4)$$

where T and V denote the kinetic and potential contributions respectively. To these densities, one can associate their corresponding energy density parameters, and their sum $\Omega_\phi = \Omega_T + \Omega_V$. The dotted quantities are derivatives with respect to the cosmic time t, while $\phi' = \frac{d\phi}{d\ln a}$ denotes derivatives with respect to the logarithm of the scale factor, and $\partial_\tau\phi = (aH)\phi'$ for derivatives with respect to conformal time τ.

The model's Friedmann and Klein-Gordon equations are

$$H^2 = \frac{8\pi G}{3}\rho, \qquad (5a)$$

$$\ddot{\phi} + 3H\dot{\phi} = 4\pi G\sigma, \qquad (5b)$$

where the ρ is the total density of all components of the universe (including the dilaton) and $H = \dot{a}/a$ is the usual Hubble parameter. Furthermore, the interaction of the field is described by

$$\sigma = \sigma_V + \sigma_m = -\frac{1}{8\pi G}\frac{\partial V(\phi)}{\partial\phi} + \sum_i \alpha_i(\phi)(3P_i - \rho_i), \quad (6)$$

whose first term describes the self-interactions of the dilaton from the potential, while the second term describes the dilaton couplings to the other components of the universe.[1] The index i spans all components (hadrons, dark matter, radiation…) with corresponding densities ρ_i and pressures P_i. The coupling strengths are quantified by coefficients[2] α_i given by the logarithmic gradients of their masses

---

[1]Note the perhaps surprising extra factor of $1/2$ in front of the potential derivative in the source term of the Klein-Gordon equation (5b). This is due to the definition we choose for the action of the field's potential in Eq. (2) with an unconventional $(8\pi G)^{-1}$ factor.

[2]Not to be confused with the fine-structure constant α and its value at redshift zero $\alpha(z=0) = \alpha_0$.

$$\alpha_i(\phi) = \frac{\partial \ln m_i(\phi)}{\partial \phi}. \qquad (7)$$

This field induced mass variation is a direct signature of the theory of gravity being nonmetric.

As discussed in [10], one can model the ϕ dependence of the hadron coupling α_h and dark matter coupling α_m using

$$\alpha_h(\phi) = \alpha_{h,0} e^{-(\phi - \phi_0)}, \qquad (8a)$$

$$\alpha_m(\phi) = \alpha_{m,0} e^{-(\phi - \phi_0)}, \qquad (8b)$$

where we introduced the notations $\alpha_{i,0} = \alpha_i(\phi_0)$ and $\phi_0 = \phi(z = 0)$. Doing so, the Klein-Gordon equation can be entirely described in terms of the difference $\phi - \phi_0$. The couplings to hadrons/leptons/dark matter are driving most of the late time cosmological evolution of the field. Another important interaction, albeit more speculative, is that to a model of dark energy (if not generated through the dilaton itself), through a coupling term α_{DE}. If this component behaves as a cosmological constant, we have $\sigma_{DE} = \alpha_{DE}(3P_{DE} - \rho_{DE}) \sim -4\alpha_\Lambda \rho_\Lambda$. We will only consider the case where α_Λ is a constant, which was assumed in most of the previous phenomenological studies [12–14] where α_Λ was denoted α_V. Note however that this notation was misleading, as this behavior cannot be simply created by some fine tuned potential of ϕ, but requires some interaction between the dilaton and dark-energy.

The coupling to radiation is always irrelevant, since in that case $\rho_r = 3P_r$ and the term of Eq. (6) always vanishes. The only other interaction of cosmological interest might be that with massive neutrinos, which is left for future work.

It is convenient to treat the contribution from the dilaton potential simply as another species in the σ sum, with coupling[3] $\alpha_V = \frac{1}{4}\frac{\partial \ln V}{\partial \phi}$. Note that any constant in the potential $V(\phi) = \Lambda$ adds a term to the Lagrangian equation (2) that is effectively equivalent to a cosmological constant. As such, while being conceptually different, the situation in which the runaway dilaton provides the source for dark energy with a constant potential is phenomenologically equivalent to a runaway dilaton field completely decoupled from dark energy ($V = 0$, $\alpha_\Lambda = 0$) plus a cosmological constant. However, for α_Λ to be nonzero requires that $V = 0$ and Λ to be a different source of dark energy. In addition to these two simple scenarios, we will consider the exponential potential $V(\phi) = A_x e^{c_x(\phi - \phi_0)}$, leading to $\alpha_V = c_x/4$ which represents a well motivated potential from string theory [10,11].

The field equations with the couplings as presented thus far display an attractor behavior, shown in Fig. 1. First, the initial value of the field is irrelevant in the overall evolution.

---

[3]The normalization is set to ensure consistency with the definitions in the literature [10].
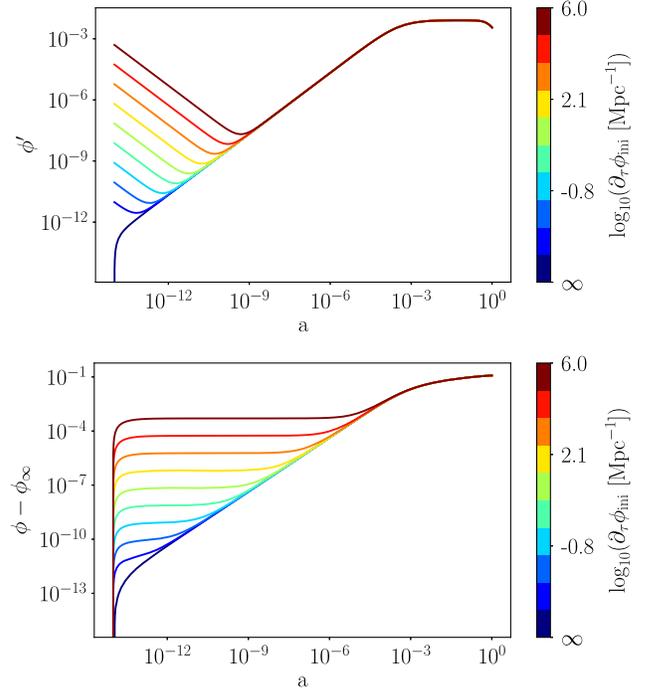
FIG. 1. Evolution of the dilaton field and its speed with respect to the scale factor for different values of its initial speed. Here $V(\phi) = 0$, $\alpha_{m,0} = -1 \times 10^{-2}$, and $\alpha_{h,0} = -1 \times 10^{-5}$.

This is naturally expected from the Eqs. (5b) and (8b) (which only depend on field differences, not the overall value). Second, there could be, in principle, a dependence on the initial velocity. We observe in Fig. 1 that due to Hubble friction the field velocity quickly decays from whatever velocity is chosen at the beginning of the evolution to the value that is forced by its interaction with massive species (the "attractor"). This causes the field ϕ to eventually reach a plateau. The overall displacement of the field from its initial value ($\phi - \phi_\infty$) can take on different values at the plateau, depending on the precise initial condition. However, for a large range of initial velocities the late time field velocity (and thus also the overall displacement) is most significant around matter domination, where the acceleration from the coupling is strongest compared to the Hubble friction. In this range the initial velocity is irrelevant. The starting redshift (here 10^{14}) is of course set arbitrarily, but this choice does not significantly impact our results.

A. Impact on observations

All the dimensionless coupling coefficients quantifying fundamental interactions of the standard model are expected to be dynamical quantities evolving with the dilaton field itself. The fine-structure constant α, quantifying the strength of the electromagnetic interaction, is for this reason expected to exhibit a dynamical behavior and will be directly proportional to the field's coupling to the

kinetic term of the Maxwell field strength F, $B_F(\phi)$ in the Lagrangian [Eq. (2)]. This is particularly relevant due to the extensive astrophysical and laboratory measurements of α.

One can show that the time evolution of α can be linked to the dilaton coupling and field speed as [10,12]:

$$\frac{1}{H}\frac{\dot{\alpha}}{\alpha_0} \approx \frac{\alpha_h(\phi)}{40}\phi', \quad (9)$$

where α_0 is today's value of the fine-structure constant. This leads to the following redshift dependence

$$\frac{\Delta\alpha}{\alpha_0}(z) := \frac{\alpha(z) - \alpha_0}{\alpha_0} = \frac{\alpha_{h,0}}{40}[1 - e^{-(\phi(z)-\phi_0)}]. \quad (10)$$

An example of this evolution for various dilaton coupling values to hadrons is given in Fig. 2.

A different value of α during big bang nucleosynthesis (BBN) also impacts the values of primordial abundances. The most significant of these is the Helium-4 fraction. One can simply model that the induced variation of $Y_{^4\mathrm{He}}$ as

$$\frac{\Delta Y_{^4\mathrm{He}}}{Y_{^4\mathrm{He}}} = \kappa_{\mathrm{BBN}}\frac{\Delta\alpha}{\alpha_0}. \quad (11)$$

For the runaway dilaton, the sensitivity coefficient κ_{BBN} is expected to be of order unity [17]. We will hence set $\kappa_{\mathrm{BBN}} = 1$ for the remainder of this work. However, we stress that the impact of this parameter on the analysis is negligibly small.

Furthermore, as discussed in [18,19], α appears in various expressions quantifying the interactions between baryons/leptons with the photons at recombination epoch.

Ultimately, the atomic energy levels of the hydrogen atoms are shifted, leading to a delay or advance of

recombination. This will impact all the interaction rates and thus, the behavior of the visibility function leading ultimately to a shift of the sound horizon at the last scattering surface, impacting the large ℓ values of the angular power spectrum of the cosmic microwave background [18,20] and the value of the Hubble parameter at high redshift [19,21,22]. We self-consistently model this variation of the α fine-structure parameter using Eq. (10).

A minor influence on the redshift of reionization is also expected to be induced by a varying α. However, the dynamics of reionization is much less known, and the impact would be far less constrained by current data. For this reason, we will ignore it in the present study.

Last but not least, string theory is not a metric theory of gravity, implying that a violation of the Einstein equivalence principle is not only expected but indeed unavoidable at some level [6]. It can be shown that the Eötvos parameter η, quantifying deviations from the universality of free fall (UFF) and the Eddington parameter γ (related to light deviation by massive objects, and constrained by the Cassini bound) are directly proportional to the square of the dilaton coupling to hadrons [10,23]. At $z = 0$, one can derive bounds from general nuclear binding energy formulas

$$\eta \simeq 5.2 \times 10^{-5}\alpha_{h,0}^2, \quad (12a)$$

$$\gamma - 1 \simeq -2\alpha_{h,0}^2. \quad (12b)$$

III. DATASETS

The runaway dilaton model can be constrained throughout the cosmic evolution using a wide range of local, astrophysical, and cosmological datasets, which we now enumerate.

Local constraints come from experiments on Earth laboratories or in low Earth orbit. Specifically, MICROSCOPE [24] provides constraints[4] on η at $z = 0$

$$\eta = (-1.5 \pm 2.7) \times 10^{-15}. \quad (13)$$

Furthermore, [25] provides laboratory constraints on the drift rate $\dot{\alpha}/(\alpha_0 H)$ at $z = 0$ using experiments based on atomic clocks, constraining a variation of the fine-structure constant at current times as

$$\frac{1}{H_0}\left(\frac{\dot{\alpha}}{\alpha_0}\right)_{z=0} = (0.014 \pm 0.015) \times 10^{-6}. \quad (14)$$

Finally, the Oklo natural nuclear reactor [26] provides a geophysical constraint on $\Delta\alpha/\alpha$
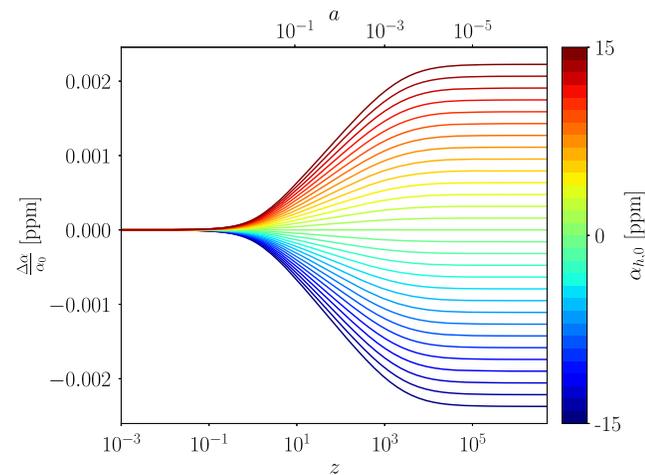
FIG. 2. $\frac{\Delta\alpha}{\alpha_0}$ as a function of z and a for different values of $\alpha_{h,0}$. The dark matter coupling is fixed to $\alpha_{m,0} = 10^{-3}$ and $\phi_{\mathrm{ini}} = \phi'_{\mathrm{ini}} = V = 0$.

[4]The standard deviation value is obtained by adding quadratically the statistical and systematic errors of [24].

$$\frac{\Delta\alpha}{\alpha_0}(z = 0.14) = (0.005 \pm 0.061) \times 10^{-6}. \quad (15)$$

Astrophysical constraints on α are provided by high-resolution spectroscopy of low-density absorption clouds along the line of sight of bright quasars, at low to intermediate redshifts ($z < 5$). We used the measurement described in [3] combined with recent measurements. All of them can be found in [27,28] with an extra point coming from the recent ESPResSO spectrograph measurement [29].

Finally, our cosmological data includes Planck constraints on CMB power-spectra, lensing [30,31], large scale structures and baryon acoustic oscillation from the BOSS DR-12 galaxy survey [32]. In order to constrain the cosmological background evolution, we will also use the supernovae of type Ia (SNIa) likelihood associated to the Pantheon dataset [33]. Finally, we also use $H(z)$ measurements coming from recent cosmic-clocks measurements [34].

IV. RESULTS

We aim to obtain constraints on the runaway dilaton model free parameters over the whole cosmic history using the datasets presented in Sec. III.

We use a modified version of the CLASS software [35] including the runaway dilaton field. The scalar field impact on background cosmology is computed by integrating the model equations to obtain $\phi(z)$. The code is also modified to consider the various impacts of a redshift dependent value of the fine-structure constant through the cosmic history. In particular, the computed $\Delta\alpha(z)/\alpha_0$ is given by Eq. (10).

In this work, we derive the constraints on the dilaton field simply for the case where the field is spatially homogeneous. However, we have also checked that for cases where the overall energy fraction of the dilaton is subdominant during most of the cosmic evolution, one does not obtain a significant impact of the dilaton field perturbations (when implementing the usual perturbed Klein Gordon equation, for example). As such, in these cases our results should generalize. Still, we leave a more detailed investigation of the dilaton perturbations for future work.

The likelihood analysis is done by sampling Monte Carlo Markov Chains (MCMC) with MontePython [36,37] directly coupled to the modified CLASS code. We consider the chains to be converged if, for all parameters, the Gelman-Rubin criterion satisfies $|R - 1| < 0.05$. Plotting is done using the GetDist software [38].

For every run, we sample over the standard cosmological parameters $\{\omega_b, \ln A_s, n_s, z_{\text{reio}}, H_0\}$, the dilaton parameters, and the nuisance parameters of the various likelihoods. The priors in all of these parameters are flat and unbounded. In order to remain concise, we will only display the contours for the dilaton parameters most of the time. Note that the values of ϕ_0 and ϕ'_0 are derived parameters and not sampled over. While not specified on the figures, their values are always expressed in units of $m_{\text{pl}}/\sqrt{4\pi}$.
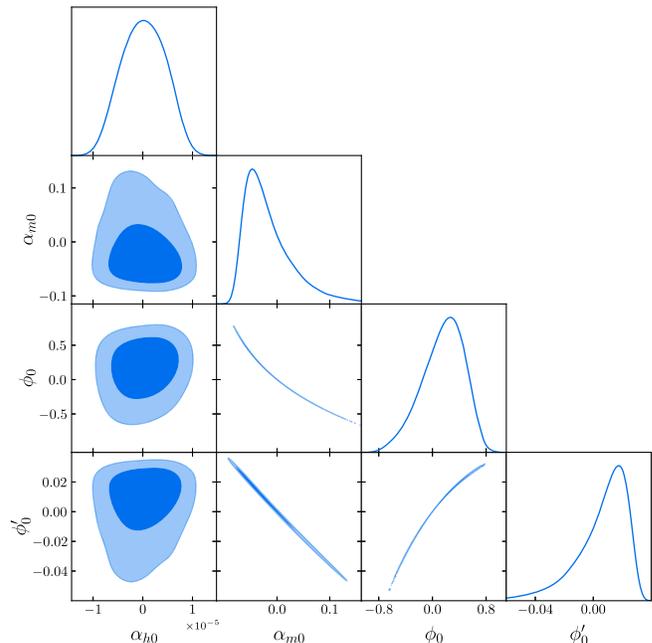
FIG. 3. Posteriors of the dilaton parameters with $\alpha_\Lambda = 0$ and a constant/zero potential.

A. Runaway dilaton and a cosmological constant

In this section we consider the cosmic evolution of a runaway dilaton model decoupled from the cosmological constant, which in this case is the only form of dark energy ($V = 0$). This is equivalent to a runaway dilaton with a constant potential $V = \Lambda$ and no cosmological constant. As such, only the dilaton couplings to baryons and/or dark matter are relevant here.

We display the 68% and 95% CL contours of the 2D marginalized posteriors for all combinations of parameters in Fig. 3 and the corresponding 68% CL are detailed in Table I. One can witness a very strong correlation between $\alpha_{m,0}$ and today's value of the field ϕ_0 and its derivative ϕ'_0, while such a correlation is mostly absent with $\alpha_{h,0}$. This is expected as the coupling to hadrons is highly constrained by local data as MICROSCOPE while the dark matter coupling, more loosely constrained by the cosmological dataset, has more freedom to accelerate the field toward late times. Compared to previous studies as [14] (which also include $\alpha_\Lambda \neq 0$), the field speed ϕ'_0 appears however to be more sharply constrained by one order of magnitude, indicating that $\alpha_{m,0}$ does not have an impact on the field evolution as strong as α_Λ (which here is fixed to 0).

B. Runaway dilaton and a constant coupling to dark energy

The latest results found in the literature (see, e.g., [14]) consider the scenario in which ϕ can be coupled to Λ with a constant coupling. In low redshift studies, an extra prior on today's field speed was given by $|\phi'_0| = 0.0 \pm 0.1$, obtained

TABLE I. Best-fit values of the runaway dilaton parameters with associated 68% confidence levels (CL) in the case $V = 0$ (or $V = \Lambda$) and $\alpha_\Lambda = 0$.

Parameter	68% CL
$\alpha_{h,0}$	$(0.24^{+4.77}_{-4.57}) \times 10^{-6}$
$\alpha_{m,0}$	$(-1.33^{+1.92}_{-6.09}) \times 10^{-2}$
ϕ_0	$(1.5^{+4.0}_{-2.4}) \times 10^{-1}$
ϕ'_0	$(5.49^{+22.9}_{-7.82}) \times 10^{-3}$

TABLE II. Best-fit values of the runaway dilaton parameters with associated 68% confidence levels (CL) in the case $V = 0$ and $\alpha_\Lambda \neq 0$.

Parameter	Prior on ϕ'_0	No prior on ϕ'_0
$\alpha_{h,0}$	$(-1.63^{+4.33}_{-4.71}) \times 10^{-6}$	$(0.21^{+2.97}_{-2.80}) \times 10^{-6}$
$\alpha_{m,0}$	$(-1.70^{+2.08}_{-5.71}) \times 10^{-2}$	$(-1.39^{+2.65}_{-6.03}) \times 10^{-2}$
α_Λ	$(0.50^{+8.94}_{-9.39}) \times 10^{-2}$	$(-0.16^{+2.34}_{-3.65}) \times 10^{-1}$
ϕ_0	$(16.7^{+3.68}_{-2.43}) \times 10^{-1}$	$(17.5^{+4.25}_{-3.23}) \times 10^{-1}$
ϕ'_0	$(0.20^{+9.97}_{-9.98}) \times 10^{-2}$	$(3.7^{+38.4}_{-31.0}) \times 10^{-2}$

from separate constraints in [39,40]. This prior enables the simplification of the constraints coming from the probes of the cosmological background expansion and therefore provides the main (and effectively the only) constraint on today's field speed ϕ'_0. However, using such a prior on today's field speed is in principle unjustified for a full cosmological study since it is derived from rough assumptions (such as matter domination in the current cosmological era), which can be superseded with our likelihood sets.

We show the results without this prior as the red contours in Fig. 4, and the results with the prior on ϕ'_0 as blue contours. We further quantify the results in Table II. These results provide for the first time a study of the full model including $\alpha_{m,0}$ without making any simplifying assumptions (which were called dark, field, and matter coupling in the previous studies [12–14]). We find an improvement of the constraints on $\alpha_{h,0}$ by one order of magnitude compared to [14], solely due to the latest MICROSCOPE constraint.
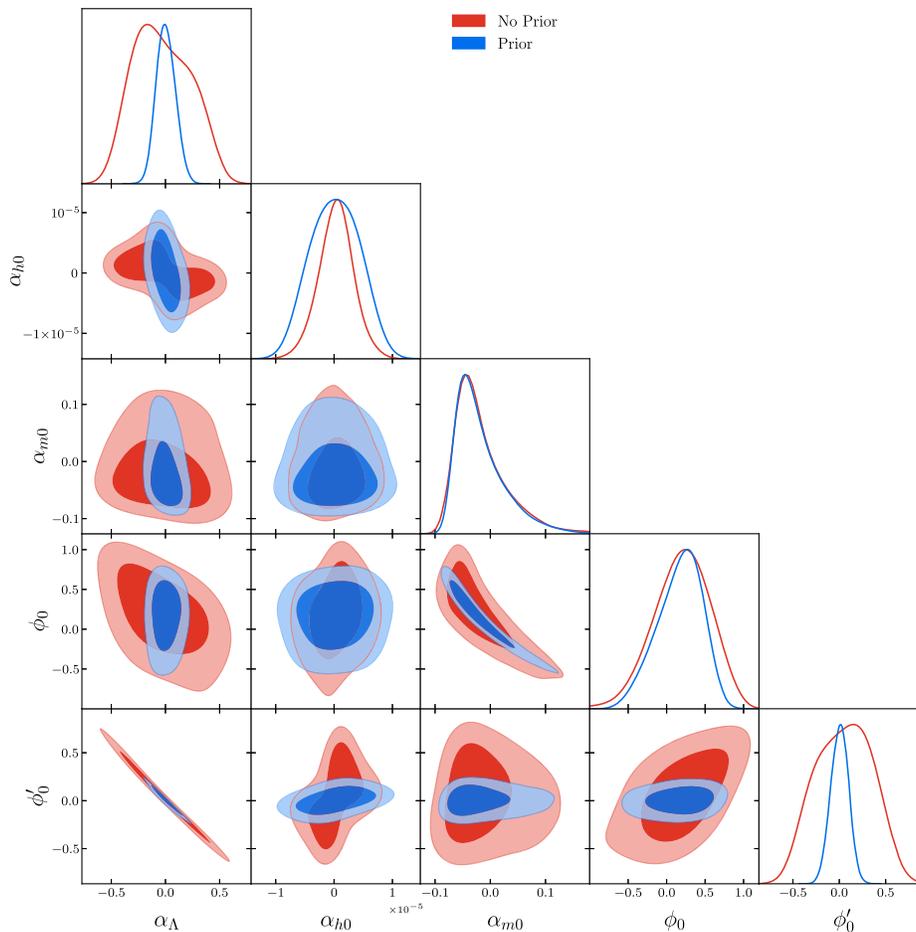
FIG. 4. Posteriors of the dilaton parameters with a constant coupling to dark energy α_Λ with an extra prior on ϕ'_0 (blue) and without it (red).
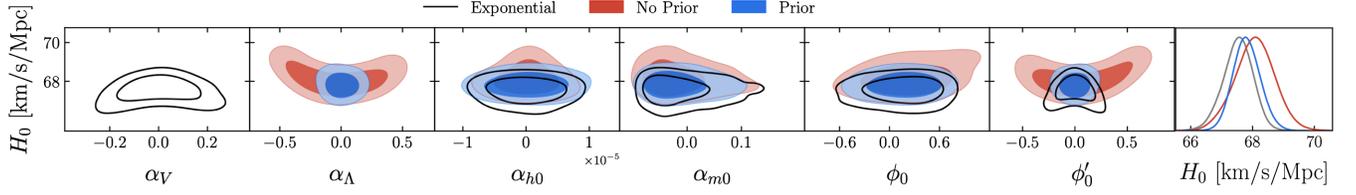
FIG. 5.   Contour plots of H_0 and the dilaton parameters in the cases of an exponential potential (black) and a constant coupling to dark energy α_Λ with an extra prior on ϕ_0' (blue) and without it (red).

The constrains on the coupling to dark energy α_Λ are identical when using the prior, as they are an indirect consequence of this restriction set on the field speed, due to the strong degeneracy one can witness between the two parameters.

While α_m guides the field evolution in matter domination (and thus has a strong impact on the overall field offset ϕ_0) the impact of the dark energy coupling α_Λ is much stronger at late times (around dark energy domination), leading to a very tight degeneracy between α_Λ and the current field speed ϕ_0'.

When leaving the prior, the contours are even more non-Gaussian, allowing for large values of α_Λ and hence of the field speed. Surprisingly, the coupling $\alpha_{h,0}$ appears to be ~ 2 times more constrained without providing any prior on ϕ_0', below what the MICROSCOPE bound [Eq. (13)] can constrain. This is a result from a Bayesian projection effect: The larger space of ϕ_0' allowed also allows for a greater amount of models close to $\alpha_{h,0} \sim 0$ to be viable [due to the atomic clock likelihood constraining only the product $\alpha_{h,0}\phi_0'$, see Eqs. (9) and (14)]. This, in turn, explains the specific shape of the contour in the $(\phi_0', \alpha_{h,0})$ space asking for the two parameters to have the same sign for their product to be positive, and tightens the posterior around $\alpha_{h,0}$ from the Bayesian marginalization.

Since we do not have any potential in this case, the overall energy density of the field [Eq. (3)] is solely given
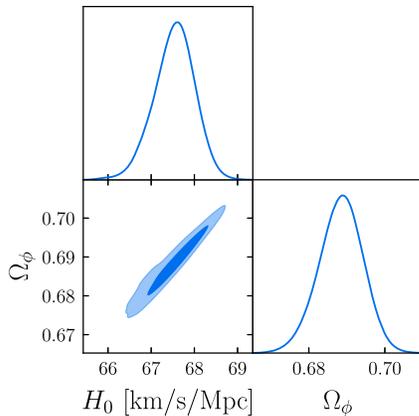
by the kinetic energy of the field ($\Omega_\phi = \Omega_T$). Given that a large coupling to Λ is allowed ($|\alpha_\Lambda| \gg 0$), we find that the field strongly accelerates at late times, leading to $d\rho_\phi/d\ln a > 0$ (and large $|\phi_0'|$). This naturally allows for a higher H_0 due to the geometrical degeneracies in the CMB (compare, e.g., with a model of dark energy equation of state with $w < -1$).[5] The contour plots relating the dilaton parameters and H_0 are displayed in Fig. 5. We can observe that today's value of the Hubble parameter H_0, is impacted quite strongly by high values of ϕ_0'. Releasing the prior on ϕ_0' naturally allows for higher H_0 values: $H_0 = 68.2^{+0.51}_{-0.65}$ km/s/Mpc   instead   of $H_0 = 67.8 \pm 0.43$ km/s/Mpc with the prior. These conclusions could be relevant in the context of the ~ 4–5σ observational tension on the value of H_0 and the theoretical limitations of Λ as the standard source of dark energy (see, e.g., [41]). We observe, however, that (due to the atomic clock bound) this quintessencelike behavior of the dilaton field in this configuration is only allowed for smaller values of $\alpha_{h,0}$ and hence smaller violations of general relativity. A targeted and complete study on the role of the dilaton field in this regard remains for future work.

C. Exponential potential

We will now consider the case of an exponential shape for $V(\phi)$. In this case the runaway dilaton potential can explain all of the dark energy in the universe, providing that we add a constant term to V. The contours are shown in Fig. 7, and the corresponding constraints are displayed in Table III. As expected, we obtain a high value for

---

[5]The equation of state of the dilaton naturally always obeys $w_\phi > -1$ since $1 + w_\phi = 2\dot\phi^2/[\dot\phi^2 + V(\phi)] > 0$. However, since we have $d\rho/d\ln a > 0$ this is effectively equivalent to a decoupled species with $w < -1$ since for such a species $d\rho/d\ln a = -3(\rho + P) = -3\rho(1 + w) > 0$. The point why such a behavior is preferable can be explained by looking at how late-time solutions to the Hubble tension manage to keep the angular diameter distance (and thus the sound horizon angle) constant. Since we can write $D_A(z_*) \approx \frac{1}{H_0}\int_0^{z_*} dz/\sqrt{\Omega_\phi(z) + \Omega_\Lambda + \Omega_m(1 + z)^3}$, if we increase H_0 it is important to decrease the integrand and thus $\Omega_\phi(z)$ in order to keep $D_A(z_*)$ constant. Since $\Omega_\phi(z = 0) = 1 - \Omega_m - \Omega_\Lambda$ is fixed, this can only happen if $d\Omega_\phi(z)/dz \propto d\rho_\phi(z)/dz \propto -d\rho_\phi(z)/d\ln a < 0$.

FIG. 6.   Contour plot of Ω_ϕ and H_0 for the exponential potential scenario.
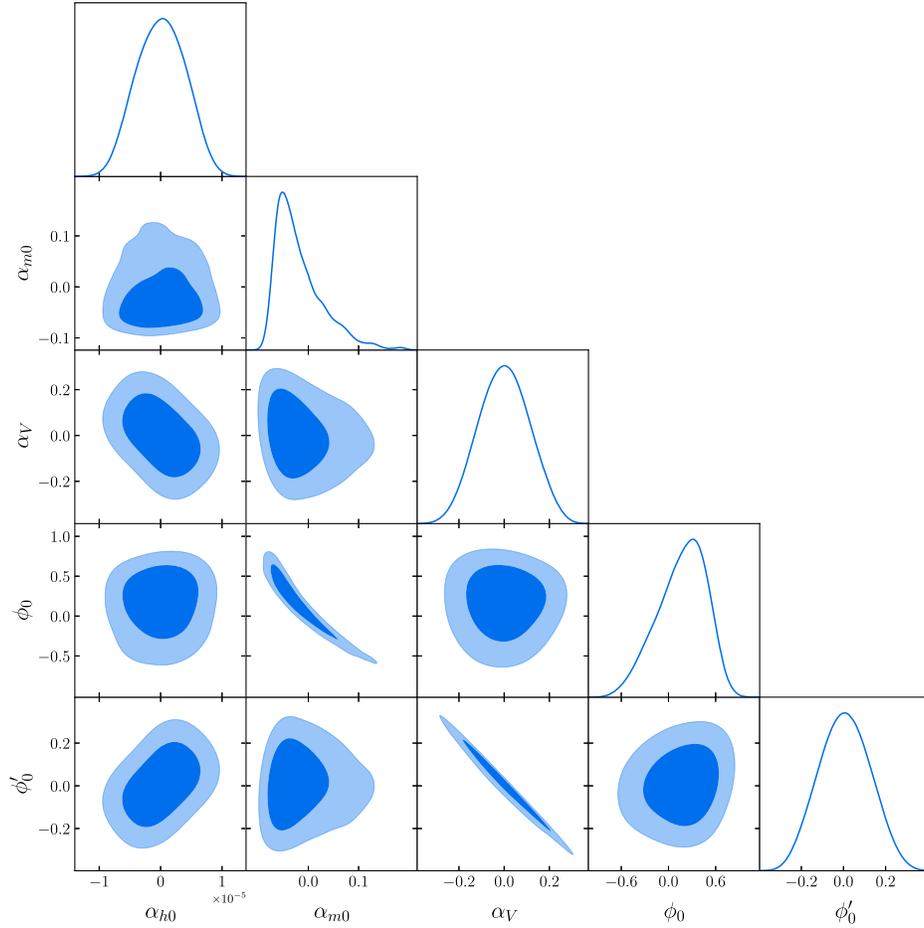
FIG. 7.   Contour plots for the dilaton parameters in the exponential potential scenario.

$\Omega_\phi = 0.688 \pm 0.006$, showing a strong degeneracy with H_0 in Fig. 6. This is expected from the measurement of the CMB sound horizon angle, which tightly constrains $\Omega_m h^3 \approx (1 - \Omega_\phi) h^3$. We also observe that this additional degree of freedom does not significantly impact the constraints on $\alpha_{h,0}$ or $\alpha_{m,0}$. In this scenario we find that H_0 cannot be increased, only decreased. Since the total field energy in this case is dominated by the potential, and one naturally finds $dV/d\ln a < 0$ (as long as $|\alpha_V| \gg 0$).[6]

Including both a coupling to a non-negligible cosmological constant and a runaway dilaton potential at the same time causes the parameter space to become extremely hard

to sample efficiently. This is because the limit of $\Lambda \to 0$ (with the dilaton potential playing the role of dark energy) naturally allows α_Λ to diverge. At the same time, the limit of small Ω_ϕ and correspondingly small $V(\phi)$ also allows the dilaton potential parameters to diverge arbitrarily. As such, instead of imposing arbitrary priors on either the coupling parameters or the cosmological densities, we do not treat this case.

TABLE III.   Best-fit values of the runaway dilaton parameters with associated 68% confidence levels (CL) for the exponential potential case.

Parameter	68% CL
$\alpha_{h,0}$	$(0.01^{+4.22}_{-4.17}) \times 10^{-6}$
$\alpha_{m,0}$	$(-1.68^{+2.24}_{-5.78}) \times 10^{-2}$
α_V	$(0.04^{+1.12}_{-1.27}) \times 10^{-1}$
ϕ_0	$(1.64^{+3.82}_{-2.53}) \times 10^{-1}$
ϕ'_0	$(0.02^{+1.36}_{-1.26}) \times 10^{-1}$

---

[6]For a field rolling down its potential one naturally expects $dV/d\ln a < 0$, but this can also be confirmed by noticing that $dV/d\ln a = dV/d\phi \cdot \phi'$ and noticing that due to Eq. (5b) the field speed ϕ' naturally evolves in the opposite direction of $dV/d\phi$, i.e., $(\phi')' \propto -dV/d\phi$ as long as the Hubble drag and the other coupling terms are comparatively negligible, we also find in this case $d\rho/d\ln a < 0$ which (comparably to a dark energy model with $w > -1$) results in lower values of H_0.

V. DISCUSSION AND CONCLUSION

The runaway dilaton model provides a general and self-consistent framework to study the stability of fundamental constants, and the cosmological impact of their space-time variations. It also allows us to probe credible models of string theories with existing datasets. In this work, we obtained the first constraints on the complete parameter space of this model, considering its full cosmological evolution with minimal assumptions on its couplings, updating and refining previous studies. To do so, we benefit from the synergy of multiple independent probes as cosmological, astrophysical, and laboratory datasets. In particular, a major lever arm is provided by the final data release of the MICROSCOPE experiment [24]. We explored three scenarios of increasing complexity, showing that order unity couplings (which would be natural in string theory) are ruled out in all cases.

While the possible field evolution is expected to be further constrained by the data of incoming wide cosmological surveys as Euclid [42], DESI [43], CMB *Stage*-4 [44], or *LiteBIRD* [45], major restriction of its parameter space are expected to be provided by future experiments allowing to directly measure the value of the fine structure constant with an extreme precision, either in laboratory with nuclear clocks [46], in the nearby universe using spectroscopy [47], or in the primeval universe with spectral distortions of the CMB [48].

Runaway dilaton models (and, more widely, all scalar field induced varying constant models) can additionally play an important role in contemporary debates triggered by the recent discovery of the accelerated expansion of the universe [49,50] and the nature of dark energy. As shown in [19,21,22,51], a redshift dependence of α—or possibly of the electron mass m_e—can have a significant impact on recombination processes that could partially ease or solve the Hubble tension. Providing a suitable choice of couplings or potential, we discussed how the runaway dilaton field can act as dynamical dark energy and significantly impact the value of H_0. Future studies will reveal if possible extensions of this model can further ease cosmological tensions or if the framework is too restrictive to feasibly do so.

[1] CMS Collaboration, Observation of a new boson at a mass of 125 GeV with the CMS experiment at the LHC, Phys. Lett. B **716,** 30 (2012).

[2] Atlas Collaboration, Observation of a new particle in the search for the Standard Model Higgs boson with the ATLAS detector at the LHC, Phys. Lett. B **716,** 1 (2012).

[3] C. J. A. P. Martins, The status of varying constants: A review of the physics, searches and implications, Rep. Prog. Phys. **80,** 126902 (2017).

[4] S. Mukhi, String theory: A perspective over the last 25 years, Classical Quantum Gravity **28,** 153001 (2011).

[5] L. Susskind, The world as a hologram, J. Math. Phys. (N.Y.) **36,** 6377 (1995).

[6] C. M. Will, The confrontation between general relativity and experiment, Living Rev. Relativity **17,** 4 (2014).

[7] C. M. Will, *Theory and Experiment in Gravitational Physics* (Cambridge University Press, Cambridge, 2017), 2nd ed.

[8] T. Damour and A. Polyakov, The string dilation and a least coupling principle, Nucl. Phys. **B423,** 532 (1994).

[9] T. Damour and K. Nordtvedt, General Relativity as a Cosmological Attractor of Tensor-Scalar Theories, Phys. Rev. Lett. **70,** 2217 (1993).

[10] T. Damour, F. Piazza, and G. Veneziano, Violations of the equivalence principle in a dilaton-runaway scenario, Phys. Rev. D **66,** 046007 (2002).

[11] M. Gasperini, F. Piazza, and G. Veneziano, Quintessence as a runaway dilaton, Phys. Rev. D **65,** 023508 (2001).

[12] C. Martins, P. Vielzeuf, M. Martinelli, E. Calabrese, and S. Pandolfi, Evolution of the fine-structure constant in runaway dilaton models, Phys. Lett. B **743,** 377 (2015).

[13] M. Martinelli, E. Calabrese, and C. J. A. P. Martins, E-ELT constraints on runaway dilaton scenarios, J. Cosmol. Astropart. Phys. 11 (2015) 030.

[14] C. Martins and L. Vacher, Astrophysical and local constraints on string theory: Runaway dilaton models, Phys. Rev. D **100,** 123514 (2019).

[15] L. Vacher, J. D. F. Dias, N. Schöneberg, C. J. A. P. Martins, S. Vinzl, S. Nesseris, G. Cañas-Herrera, and M. Martinelli, Constraints on extended Bekenstein models from cosmological, astrophysical, and local data, Phys. Rev. D **106,** 083522 (2022).

[16] R. J. Szabo, BUSSTEPP lectures on string theory, arXiv: hep-th/0207142.

[17] M. T. Clara and C. J. A. P. Martins, Primordial nucleosynthesis with varying fundamental constants. Improved constraints and a possible solution to the lithium problem, Astron. Astrophys. **633,** L11 (2020).

[18] Planck Collaboration, Planck intermediate results. XXIV. Constraints on variations in fundamental constants, Astron. Astrophys. **580,** A22 (2015).

[19] L. Hart and J. Chluba, New constraints on time-dependent variations of fundamental constants using Planck data, Mon. Not. R. Astron. Soc. **474,** 1850 (2018).

[20] S. Galli, C. J. A. P. Martins, A. Melchiorri, and E. Menegoni, Testing the variation of fundamental constants with the CMB, Astrophys. Space Sci. Proc. 22, 59 (2011).

[21] L. Hart and J. Chluba, Varying fundamental constants principal component analysis: Additional hints about the Hubble tension, Mon. Not. R. Astron. Soc. **510,** 2206 (2021).

[22] N. Lee, Y. Ali-Haïmoud, N. Schöneberg, and V. Poulin, What it takes to solve the Hubble tension through modifications of cosmological recombination, arXiv:2212.04494.

[23] T. Damour and J. F. Donoghue, FAST TRACK COMMUNICATION: Phenomenology of the equivalence principle with light scalars, Classical Quantum Gravity **27,** 202001 (2010).

[24] P. Touboul *et al.*, *MICROSCOPE* Mission: Final Results of the Test of the Equivalence Principle, Phys. Rev. Lett. **129,** 121102 (2022).

[25] R. Lange, N. Huntemann, J. M. Rahm, C. Sanner, H. Shao, B. Lipphardt, C. Tamm, S. Weyers, and E. Peik, Improved Limits for Violations of Local Position Invariance from Atomic Clock Comparisons, Phys. Rev. Lett. **126,** 011102 (2021).

[26] Y. V. Petrov, A. I. Nazarov, M. S. Onegin, V. Y. Petrov, and E. G. Sakhnovsky, Natural nuclear reactor at Oklo and variation of fundamental constants: Computation of neutronics of a fresh core, Phys. Rev. C **74,** 064610 (2006).

[27] J. K. Webb, J. A. King, M. T. Murphy, V. V. Flambaum, R. F. Carswell, and M. B. Bainbridge, Indications of a Spatial Variation of the Fine Structure Constant, Phys. Rev. Lett. **107,** 191101 (2011).

[28] M. T. Murphy and K. L. Cooksey, Subaru Telescope limits on cosmological variations in the fine-structure constant, Mon. Not. R. Astron. Soc. **471,** 4930 (2017).

[29] M. T. Murphy *et al.*, Fundamental physics with ESPRESSO: Precise limit on variations in the fine-structure constant towards the bright quasar HE 0515-4414, Astron. Astrophys. **658,** A123 (2022).

[30] N. Aghanim, Y. Akrami, F. Arroja, M. Ashdown, J. Aumont, C. Baccigalupi, M. Ballardini, A. J. Banday, R. B. Barreiro *et al.*, Planck2018 results, Astron. Astrophys. **641,** A1 (2020).

[31] Planck Collaboration, Planck 2018 results. V. CMB power spectra and likelihoods, Astron. Astrophys. **641,** A5 (2020).

[32] The B. O. S. S. Collaboration, The clustering of galaxies in the completed SDSS-III Baryon Oscillation Spectroscopic Survey: Cosmological analysis of the DR12 galaxy sample, Mon. Not. R. Astron. Soc. **470,** 2617 (2017).

[33] A. G. Riess *et al.*, Type Ia supernova distances at redshift > 1.5 from the Hubble space telescope multi-cycle treasury programs: The early expansion rate, Astrophys. J. **853,** 126 (2018).

[34] M. Moresco *et al.*, Unveiling the universe with emerging cosmological probes, Living Rev. Relativity **25,** 6 (2022).

[35] J. Lesgourgues, The cosmic linear anisotropy solving system (CLASS) I: Overview, arXiv:1104.2932.

[36] B. Audren, J. Lesgourgues, K. Benabed, and S. Prunet, Conservative constraints on early cosmology with MontePython, J. Cosmol. Astropart. Phys. 02 (2013) 001.

[37] T. Brinckmann and J. Lesgourgues, MontePython3: Boosted MCMC sampler and other features, Phys. Dark Universe **24,** 100260 (2019).

[38] A. Lewis, GetDist: A Python package for analysing Monte Carlo samples, arXiv:1910.13970.

[39] D. B. Thomas, M. Kopp, and C. Skordis, Constraining the properties of dark matter with observations of the cosmic microwave background, Astrophys. J. **830,** 155 (2016).

[40] I. Tutusaus, B. Lamine, A. Blanchard, A. Dupays, Y. Rousset, and Y. Zolnierowski, Dark sectors of the Universe: A Euclid survey approach, Phys. Rev. D **94,** 123515 (2016).

[41] J. Martin, Everything you always wanted to know about the cosmological constant problem (but were afraid to ask), C.R. Phys. **13,** 566 (2012).

[42] M. Martinelli *et al.*, Euclid: Constraining dark energy coupled to electromagnetism using astrophysical and laboratory data, Astron. Astrophys. **654,** A148 (2021).

[43] DESI Collaboration, The DESI experiment part I: Science, targeting, and survey design, arXiv:1611.00036.

[44] CMB-S4 Collaboration, CMB-S4 science case, reference design, and project plan, arXiv:1907.04473.

[45] LiteBIRD Collaboration, Probing cosmic inflation with the LiteBIRD cosmic microwave background polarization survey, Prog. Theor. Exp. Phys. **2023,** 042F01 (2022).

[46] P. Fadeev, J. C. Berengut, and V. V. Flambaum, Sensitivity of ^{229}Th nuclear clock transition to variation of the fine-structure constant, Phys. Rev. A **102,** 052833 (2020).

[47] J. Liske, G. Bono, J. Cepa *et al.*, Top level requirements for ELT-HIRES, Technical Report No. Document ESO 204697 Version 1, 2014.

[48] L. Hart and J. Chluba, Using the cosmological recombination radiation to probe early dark energy and fundamental constant variations, Mon. Not. R. Astron. Soc. **519,** 3664 (2023).

[49] A. G. Riess *et al.*, Observational evidence from supernovae for an accelerating universe and a cosmological constant, Astron. J. **116,** 1009 (1998).

[50] S. Perlmutter *et al.*, Measurements of Ω and Λ from 42 high-redshift supernovae, Astrophys. J. **517,** 565 (1999).

[51] N. Schöneberg, G. F. Abellán, A. Pérez Sánchez, S. J. Witte, V. Poulin, and J. Lesgourgues, The H_0 olympics: A fair ranking of proposed models, Phys. Rep. **984,** 1 (2022).